Zootaxa 5802 (2): 303–322
https://www.mapress.com/zt/

Article

ISSN 1175-5326 (print edition)
ZOOTAXA
ISSN 1175-5334 (online edition)

https://doi.org/10.11646/zootaxa.5802.2.4
http://zoobank.org/urn:lsid:zoobank.org:pub:B6C92F45-1D47-4CA5-9E2F-97313430B8CA

Revisiting *Colobura* (Lepidoptera: Nymphalidae): Using integrative taxonomy to identify a new species, *C. cryptica* sp. nov., and revise geographic boundaries

ANISHA SAPKOTA[1*], ANDRÉS ORELLANA[2,3], NICK V. GRISHIN[4,5], ISIDRO CHACÓN[6], DANIEL H. JANZEN[7], WINNIE HALLWACHS[7], LEINA SONG[4], SAJAN KC[1] & KEITH R. WILLMOTT[1,8]

[1]*McGuire Center for Lepidoptera and Biodiversity, Florida Museum of Natural History, University of Florida, Gainesville, FL, USA*
anishasapkota363@gmail.com; https://orcid.org/0000-0002-4351-6213
kwillmott@flmnh.ufl.edu; https://orcid.org/0000-0002-9228-0219
sajankc143@gmail.com; https://orcid.org/0000-0002-2749-0738
[2]*Departamento de Ingeniería de Producción Animal, Universidad Nacional Experimental del Táchira, Av. Universidad, Paramillo, San Cristóbal 5001-A, Táchira, Venezuela*
[3]*Fundación Entomológica Andina, Calle Urdaneta, Ejido 5111, estado Mérida, Venezuela*
aorell@unet.edu.ve; https://orcid.org/0000-0003-2358-5956
[4]*Department of Biophysics, University of Texas Southwestern Medical Center, Dallas, Texas, USA*
Leina.Song@UTSouthwestern.edu; https://orcid.org/0000-0002-1706-9376
[5]*Department of Biochemistry, University of Texas Southwestern Medical Center, Dallas, Texas, USA*
grishin@chop.swmed.edu; https://orcid.org/0000-0003-4108-1153
[6]*BioAlfa, Guanacaste Dry Forest Conservation Fund, Museo Nacional Santo Domingo de Heredia, Costa Rica*
boconera@gmail.com; https://orcid.org/0000-0001-5139-2073
[7]*Department of Biology, University of Pennsylvania, Philadelphia, PA, United States*
djanzen@sas.upenn.edu; https://orcid.org/0000-0002-7335-5107
whallwac@sas.upenn.edu; https://orcid.org/0000-0002-5166-809X
[8]*Instituto Nacional de Biodiversidad, Quito, Ecuador*
**Corresponding author*

Abstract

The Neotropical butterfly genus *Colobura* Billberg, 1820 (Nymphalidae) includes widespread, common and conspicuous species whose taxonomy one might expect to be well understood. Using integrative taxonomy—combining morphology (genitalia, larval traits, adult wing patterns, and UV reflectance), genome sequencing (mitochondrial barcodes, complete mitogenomes, and nuclear genomes), and life history data—we describe *Colobura cryptica* Sapkota, Orellana & Willmott **sp. nov**., a new species previously conflated with *Colobura annulata*. Key diagnostic morphological traits include: (1) a shorter third submarginal line on the ventral forewing that does not reach the pale cream transverse band, and (2) velvet-black larvae that lack yellow rings between segments or yellow spots at anterior edge of segments. Phylogenomic analyses resolved four distinct clades, with *C. cryptica* forming a genetically divergent lineage that is broadly sympatric with its sister species *C. annulata*. We further demonstrate a biogeographical split in *C. dirce* populations across the Andes and redefine the ranges of *C. dirce wolcotti* and *C. dirce dirce*. Genome sequencing showed that *C. d. wolcotti*, previously thought to be restricted to the Caribbean Islands, is also present in Central America and coastal Ecuador/northern Colombia west of the Andes, whereas *C. d. dirce* occurs only east of the Andes. This division corresponds with differences in ventral UV reflectance, which is strongly expressed in *C. d. wolcotti* but reduced in *C. d. dirce*. We conducted a preliminary investigation of UV-reflectance on the ventral wings and found evidence for differences across the four taxa, and we discuss the possibility of UV-mediated reproductive isolation that might have contributed to speciation in *Colobura*.

Key words: Neotropical diversification, cryptic phenotype, species delimitation, sympatric speciation, UV reflectance

Introduction

Colobura Billberg, 1820 (Lepidoptera: Nymphalidae) is a widespread Neotropical butterfly genus with only two currently recognized species. These butterflies display intricate black patterns on a cream-colored ventral wing surface, a potential cryptic adaptation enabling them to blend with tree bark in dense forest habitats, where they

Accepted by C. Prieto: 25 Mar. 2026; published: 4 May 2026

habitually perch upside down on trunks with closed wings (pers. obs.). Historically, this highly distinctive wing pattern perhaps led to the genus being considered as monotypic, with *C. dirce* (Linnaeus, 1758) as the sole recognized species until the description of *C. annulata* Willmott, Constantino & J. Hall (Willmott *et al*. 2001). The recognition of *C. annulata* as a new species was initially stimulated by larval phenotypic characters; the fifth-instar larva is velvet-black, with both species exhibiting yellow elongate lateral spots at the anterior edge of each abdominal segment; however, *C. annulata* additionally has creamy-yellow rings around each abdominal segment (Fig. 1a–b). In adults, the third submarginal line from the edge of the ventral forewing in *C. annulata* is of uniform width, unlike that in *C. dirce*, which broadens posteriorly (Willmott *et al*. 2001) (Fig. 2a–b). Additionally, there is evidence of differing larval niches: *C. dirce* larvae feed on the foliage of young *Cecropia* Loefl. (Urticaceae) trees or saplings, with eggs deposited in small clusters of 2–10 individuals, whereas *C. annulata* larvae predominantly occupy mature *Cecropia* canopy trees, with eggs deposited in large clusters of up to 70 individuals (Willmott *et al*. 2001). This ecological segregation potentially correlates with adult flight height preferences (Willmott *et al.* 2001), suggesting a mechanism for reproductive isolation that may have facilitated speciation between these closely related species.

FIGURE 1. Fifth instar larva of a. *Colobura dirce*, b. *Colobura annulata*, c. *Colobura cryptica* **sp. nov.** (Photos taken from www.inaturalist.org, photo credit clockwise © Alexis López Hernández, © Daniel M. Small, © Andrés Orellana, © Andrés Orellana, © Olivier Claessens, ©Keith R. Willmott)

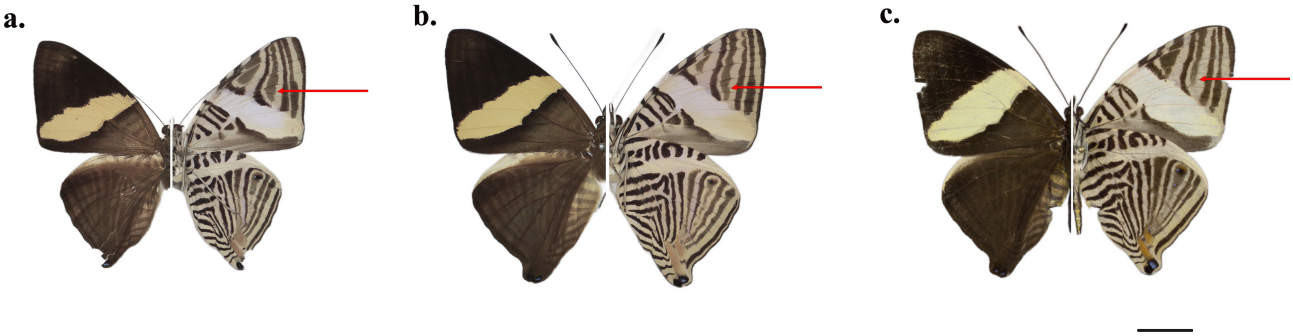

FIGURE 2. Adult specimen with arrows indicating identification keys a. *Colobura dirce* (Neotype, French Guiana: "Guyane Française C. Bar/Ex. Oberthür Coll. Brit. Mus. 1927–3." NHMUK), b. *Colobura annulata* (Holotype, French Guiana: Cayenne: "Cayenne/Ex. Oberthür Coll. Brit. Mus. 1927–3.," NHMUK), c. *Colobura cryptica* **sp. nov.** (Holotype, Ecuador: Napo. To be deposited in INABIO)

Recently, the second co-author, AO, observed a distinctive caterpillar phenotype on a *Cecropia* tree, without any characteristic yellow rings or lateral spots, which matched neither of the described species and served as the impetus for this study (Fig. 1c). An initial examination of DNA barcode data available for *Colobura* in BOLDSystems (2025) (www.boldsystems.org) showed four Barcode Index Number (BIN) clusters for this genus. Each cluster is a system-generated operational taxonomic unit (OTU) based on DNA barcode sequence similarity (Ratnasingham and Hebert, 2013) (Fig. 3). Specimens from clusters 1 and 2 aligned morphologically with adult *C. dirce*, while those from clusters 3 and 4 corresponded to adult individuals previously identified as *C. annulata*. Vouchers of cluster 4 differ consistently from the holotype of *C. annulata* in having the third submarginal line from the ventral forewing distal margin being short and not reaching the transverse pale band (Fig. 2c). This is a potentially notable character, given that the shape of this same submarginal line also distinguishes *C. annulata* from *C. dirce*. Therefore, the primary objective of this study was to examine the significance of these larval, wing pattern and DNA sequence differences to determine whether they are the result of unrecognized additional species within the genus.

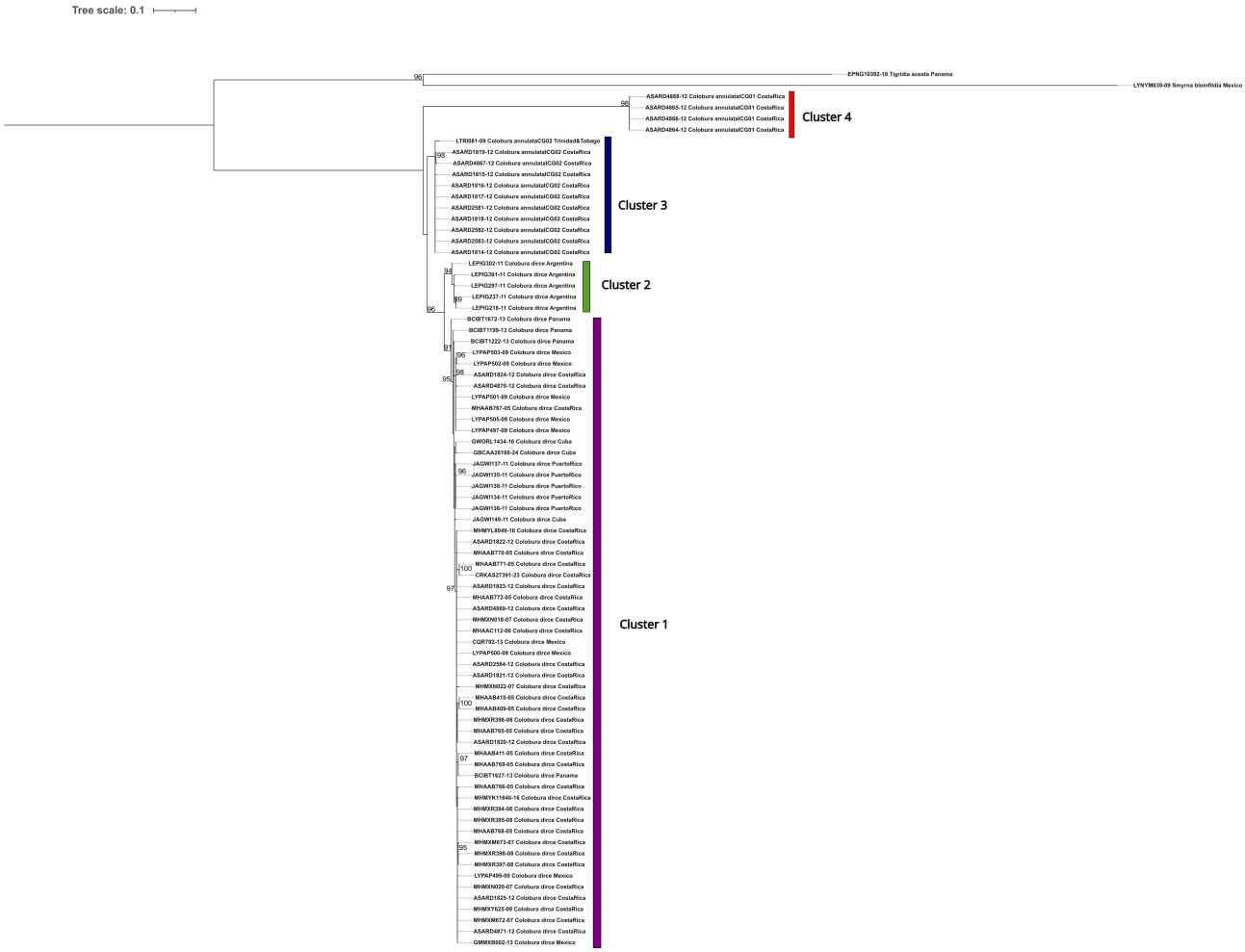

FIGURE 3. Phylogenetic tree for *Colobura* constructed using the barcode region of the mitochondrial gene COI.

Additionally, while examining museum specimens for this study, we also noticed a striking variation in UV reflectance on the ventral wings among *C. dirce* individuals. Butterflies detect and utilize UV signals for species recognition and mate selection (Silberglied and Taylor, 1978; Briscoe *et al.* 2010), with population-level UV expression influenced partly by climatic factors (Obara *et al*. 2008; Fenner *et al*. 2019). In *C. dirce*, this variation appears to follow distinct geographical clines: UV reflectance is strongly expressed in Caribbean populations, highly variable from Mexico to Panama and in coastal Ecuador/northern Colombia west of the Andes and markedly reduced or absent in populations east of the Andes. Interestingly, BOLDSystems (2025) grouped *C. dirce* specimens from Central America in Cluster 1 and those from Brazil and Argentina in Cluster 2 (in different BINs) (Fig. 3), raising the possibility that the Andes may have acted as a biogeographical barrier promoting divergence in this species.

Building on this, we also sought to examine UV reflectance properties in other *Colobura* species, particularly to determine whether sympatric taxa exhibit distinct UV reflectance patterns. Consequently, a secondary objective of this study was to investigate UV reflectance across *Colobura* species and evaluate its potential role in speciation.

We employed integrative taxonomy to investigate these questions (Dayrat 2005; Schlick-Steiner *et al.* 2010), combining three sources of data: morphological examinations of external and genital structures including study of UV reflection properties of wings; molecular analyses (including DNA barcoding, complete mitochondrial genome sequencing and nuclear genome assessment of both Z-chromosomes, particularly valuable for species delimitation (Cong *et al*. 2019), and autosomal chromosomes); and life history data.

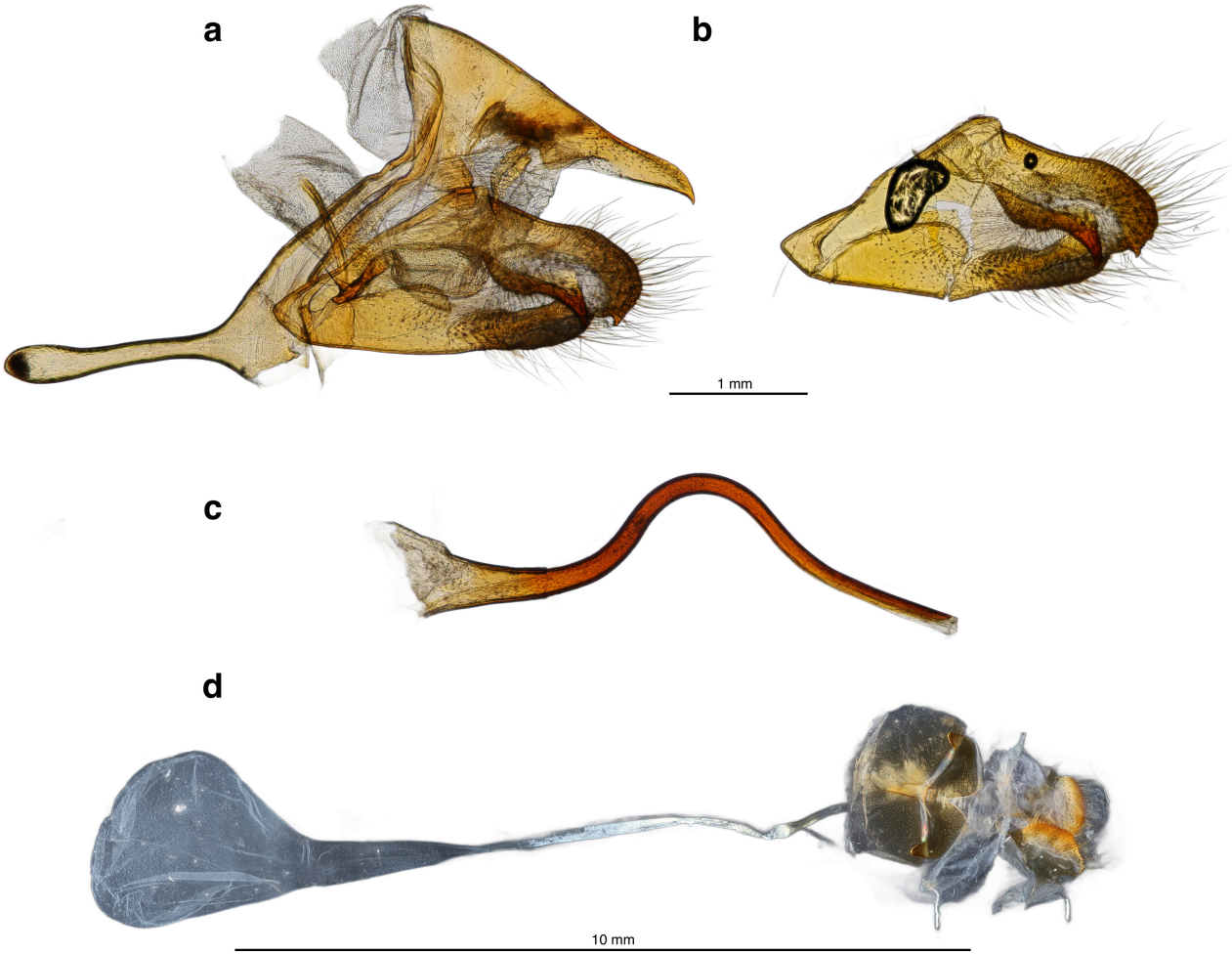

FIGURE 4. Male and female genitalia of *Colobura dirce dirce* a. lateral view of male genitalia with aedeagus removed, b. inner lateral view of valva, c. lateral view of aedeagus d. dorsal view of female genitalia (reference scale: 1 mm for male genitalia, 10 mm for female genitalia).

Methods

The following acronyms are used for collections mentioned in this study:

AOP—Andrés Orellana Private Collection, San Cristóbal, Táchira State, Venezuela
FSCA—Florida State Collection of Arthropods, Gainesville, Florida, USA
FUNEA—Fundación Entomológica Andina Collection, Ejido, estado Mérida, Venezuela
INABIO—Instituto Nacional de Biodiversidad, Quito, Ecuador
INBio—Instituto Nacional de Biodiversidad, Costa Rica
MGCL—McGuire Center for Lepidoptera and Biodiversity, Florida Museum of Natural History, University of Florida, Gainesville, Florida, USA

NHMUK—The Natural History Museum, London, United Kingdom
NMNH—Smithsonian Institution, National Museum of Natural History, Washington, D.C., USA
QCAZ—Museo de Zoología, Sección Invertebrados, Pontificia Universidad Católica, Quito, Ecuador
TAMU—Texas A&M Biodiversity Research and Teaching Collections, College Station, Texas, USA

For this study, we examined museum specimens (adults), freshly collected material (adults) and photographs available from iNaturalist (2025) (both adults and larva). All available *Colobura* specimens (n=670) from the MGCL were curated and divided into four morphological groups: (1) *C. dirce* with strong ventral UV reflectance, (2) *C. dirce* with reduced or absent ventral UV reflectance, (3) typical *C. annulata*, and (4) *C. annulata* specimens displaying a shorter third submarginal line that does not reach the transverse creamy-yellow band on the ventral forewing surface. Holotype labels were transcribed exactly as written, using a single slash "/" for a new line, double slashes "//" for a new label, square brackets "[ ]" to indicate label color, and parentheses "()" to indicate specimen voucher number and sex. Paratype labels were transcribed in a structured format listing country, region, locality, date, collector, collection or museum ID, DNA voucher (when available), geographic coordinates, elevation, and specimen number with sex in parentheses, with multiple specimens from the same locality separated by semicolons and additional notes (e.g., "dissected" or "failed") included in parentheses.

Morphology study: External and genital morphology were examined for all clusters. To study leg morphology, the structures were immersed in concentrated sodium hypochlorite solution (99%) for at least 3 minutes to clear the scales (the scales were highly hydrophobic). The structures were then studied using a Leica stereomicroscope (Model MZ 16). The structures were rinsed afterwards and stored in a capsule with the corresponding specimen. For each cluster, both males and females (at least two specimens of each sex) were examined. For wing venation, wings (left or right) were immersed in sodium hypochlorite solution for 6–7 minutes, and any remaining scales were gently removed with a paintbrush. Wing venation was studied for one male specimen per cluster.

Genitalia Preparation and Imaging. At least two male and two female genitalia from each group were dissected by soaking abdomens in 10% KOH overnight at room temperature, followed by clearing in water using fine forceps, No. 2 entomological pins, and a pointed sable brush. The clean genitalia (without scales or attached tissue) were mounted in glycerin on watch glasses and photographed at FSCA using a Macropod imaging system equipped with a Canon EOS 6D Mark II camera and a Canon MP-E 65 mm macro lens. One genitalia image was taken using a Canon EOS 70D camera attached to an Olympus BX51 compound microscope under a 10x objective lens. Canon EOS Utility 3.14.30.4 and Helicon Focus® Pro 7.7.5 were used for focus stacking. Image post-processing was done using Photopea (https://www.photopea.com/) and Preview application on macOS (Version 11.0). Genitalia from each specimen, identified by a unique genitalic vial number on the specimen label, were preserved in separate vials in glycerin for future reference. The dissected specimens are specified in the Material Examined section in parentheses.

Distribution maps and external morphology. Location data were gathered from the MGCL collection, AO, and iNaturalist (www.inaturalist.org). Geographic point data were visualized using SimpleMappr (www.simplemappr.net) (Shorthouse, 2010).

Molecular Work and phylogenetic tree construction. A total of 95 specimens of *Colobura* (see Supplement 1 for additional information) were selected from throughout the range of the genus, from specimens available at the MGCL, TAMU, and NMNH. At least one full leg, but generally two legs, of the dried specimens were removed for DNA extraction. The specimens were collected from the 1950s to 2024. We used the protocol of Cong *et al*. (2021), which has been proven to work well for DNA extraction from museum specimens of any age. This approach sequences each extracted DNA fragment rather than relying on amplification, making it effective for old museum specimens, whose DNA is often fragmented into 30–50 bp segments (Zhang *et al*. 2024). The DNA was fragmented to 150 base pairs or shorter and then sequenced using the Illumina next-generation sequencing platform. The resulting sequence data were used to construct exons of protein-coding genes, guided by the reference genome of *Heliconius melpomene* (Linnaeus, 1758) (Davey *et al*. 2016), which served as the basis for inferring phylogenetic trees. The barcode region of the mitochondrial cytochrome oxidase I (COI) gene was sequenced for select specimens using methods outlined by Willmott *et al*. (2017) to verify identification of specimens and help identify diagnostic characters. Remaining barcode sequences were obtained from BOLDSystems (www.boldsystems.org), retaining only *Colobura* specimens with complete 658-bp sequences. *Tigridia acesta* (Linnaeus, 1758) and *Smyrna blomfildia* (Fabricius, 1781) were used as outgroups, both of which are in the tribe Nymphalini

(as is *Colobura*) and are phenotypically similar (Chazot *et al*. 2019). Four separate trees were generated using IQ-tree v1.6.12, utilizing the GTR+GAMMA model (Nguyen *et al*. 2015): one tree was derived from autosomes in the nuclear genome, another from genes predicted to be in the Z chromosome, the third from the whole mitochondrial genome, and the fourth from the barcode region of the mitochondrial gene COI. For reconstructing the nuclear tree, 100,000 codons were randomly chosen for more efficient computation, representing 2% of the total data. A subset of 10,000 codons was again randomly selected, and the process was repeated 100 times, and the values above the node (0 to 100) of each tree show the number of times the same structure was found in the replicate analyses. Phylogenetic trees were visualized, rotated, and colored with FigTree V1.4.4 and Interactive Tree of Life (iTOL: Interactive Tree Of Life). The length of each horizontal branch of the phylogenetic tree is proportional to the number of estimated changes in DNA (i.e., fixed mutations) that occur along the branch. The length of the scale bar at the bottom of each tree corresponds to the branch length, for example, 2 changes per 100 base pairs (=0.02, or 2%). Whole genome shotgun data for each specimen are deposited in the NCBI database (https://www.ncbi.nlm.nih.gov/), and the DNA barcode data are deposited in Genbank (https://www.ncbi.nlm.nih.gov/genbank/). For each specimen in tree figures, the following information is provided (separated by "|"): taxon name, DNA sample code, sex, general locality, and year of collection, and depository.

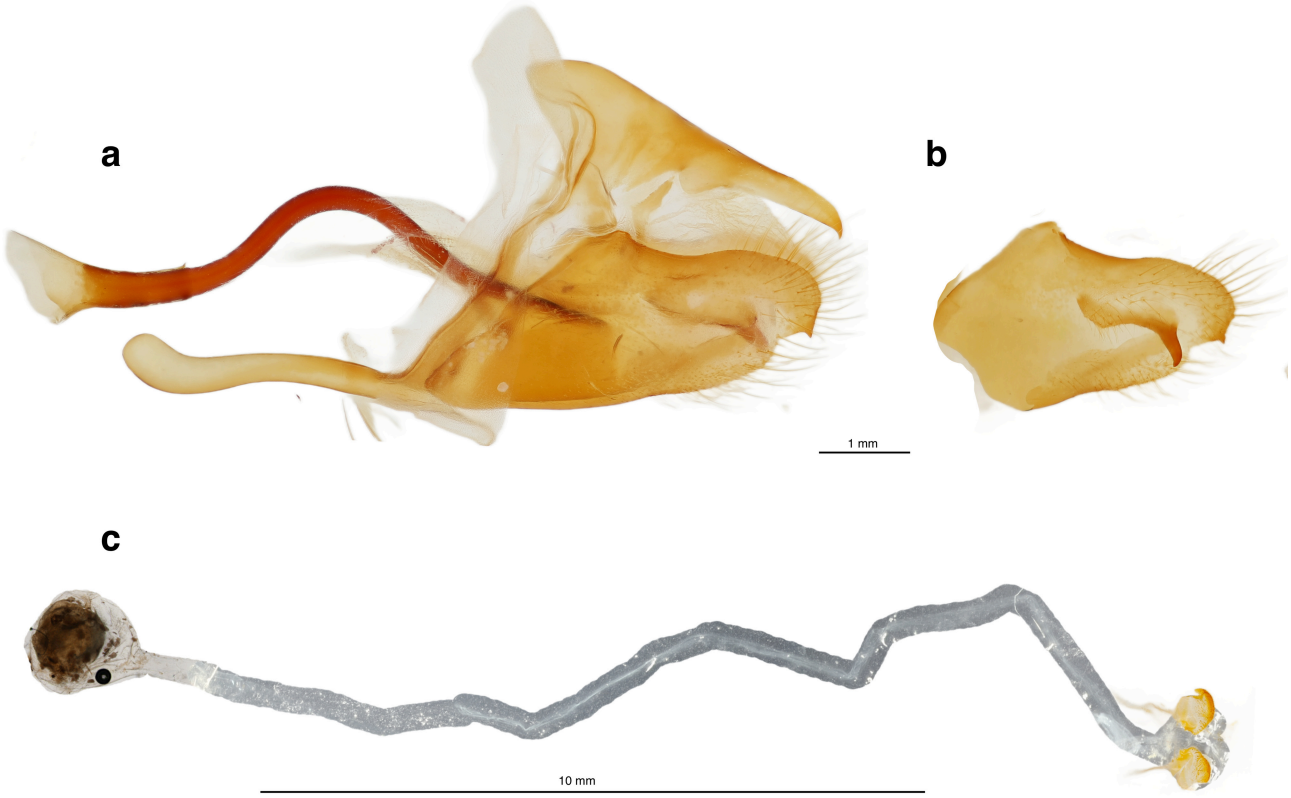

FIGURE 5. Male and female genitalia of *Colobura dirce wolcotti* a. lateral view of male genitalia with aedeagus, b. inner lateral view of valva, c. dorsal view of female genitalia (reference scale: 1 mm for male genitalia, 10 mm for female genitalia).

Life history. AO discovered a gregarious batch of caterpillars (30 individuals) on a young *Cecropia* tree about 4 m tall, growing in a small patch of secondary growth within mature humid premontane forest in Parque Paramillo, San Cristóbal, Táchira, Venezuela (1100 m; 7.7931°N, -72.1949°W). The caterpillars were located approximately 3–4 m above the ground, clustered under a leaf exhibiting the characteristic "closed umbrella" effect caused by the caterpillars chewing through primary veins. AO used a net to bring the caterpillars down and cut the entire leaf from its stalk for collection. The immatures were kept in AO's laboratory at the same location in a plastic container measuring approximately 43 × 30 × 18 cm. Inside the container, a 2.5 cm plastic mesh was arched to keep host plant material elevated above the bottom and avoid contact with frass, while also serving as a pupation substrate. Most caterpillars pupated on the mesh, though a few pupated on the underside of the container lid. Pupae on the mesh and lid were transferred to an emergence cage; those on the lid were carefully detached by lifting the silk pads and pinned to a wall to maintain an upright, natural position.

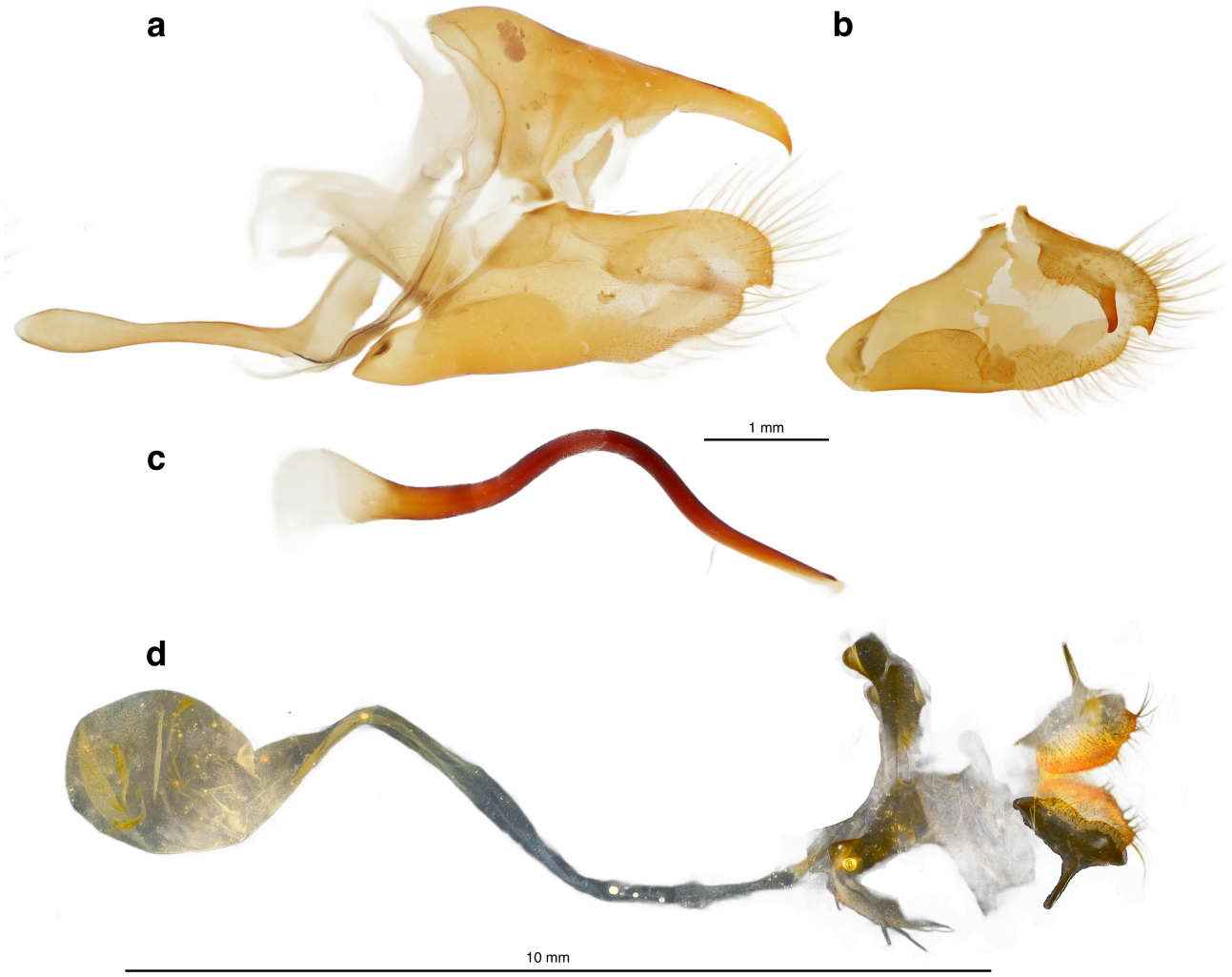

FIGURE 6. Male and female genitalia of *Colobura annulata* a. lateral view of male genitalia with aedeagus removed, b. inner lateral view of valva, c. lateral view of aedeagus, d. dorsal view of female genitalia (reference scale: 1 mm for male genitalia, 10 mm for female genitalia).

UV reflectance measurement: To obtain the UV reflectance measurements we used specimens (both males and females) whose species identifications were confirmed by genomic data and available at MGCL. A fixed spot on the ventral surface of the right hindwing, within the discal cell region, was selected due to its visible reflectance under normal daylight conditions. Measurements were performed using an integrated probe system: one fiber optic cable connected to an Ocean Insight Pulsed Xenon Light Source (PX-2) and another to an Ocean Optics Ocean SR Compact Spectrometer, while the third end of the probe both illuminated the specimen and captured reflected light. A 99% white standard was used as a reference for maximum reflectance, while a black standard was recorded with the xenon light turned off. Reflectance data were obtained using OceanView Spectroscopy software (2019). The data were visualized using RStudio Version 2025.05.1+513. Spectral data were recorded from 200–900 nm, with only the 300–700 nm range used for analysis and graphing. Measurements were taken with the wing surface flat at a 0° incident angle. Additional angles were not tested due to clear visibility at 0° and limitations of laboratory equipment. This non-invasive method preserved specimen integrity. A Kruskal-Wallis test was used to compare peak UV wavelengths among species because the spectral data did not meet the assumptions of normality and homogeneity of variance, and sample sizes were unbalanced across taxa. We used Dunn's post hoc test to identify pairwise contrasts.

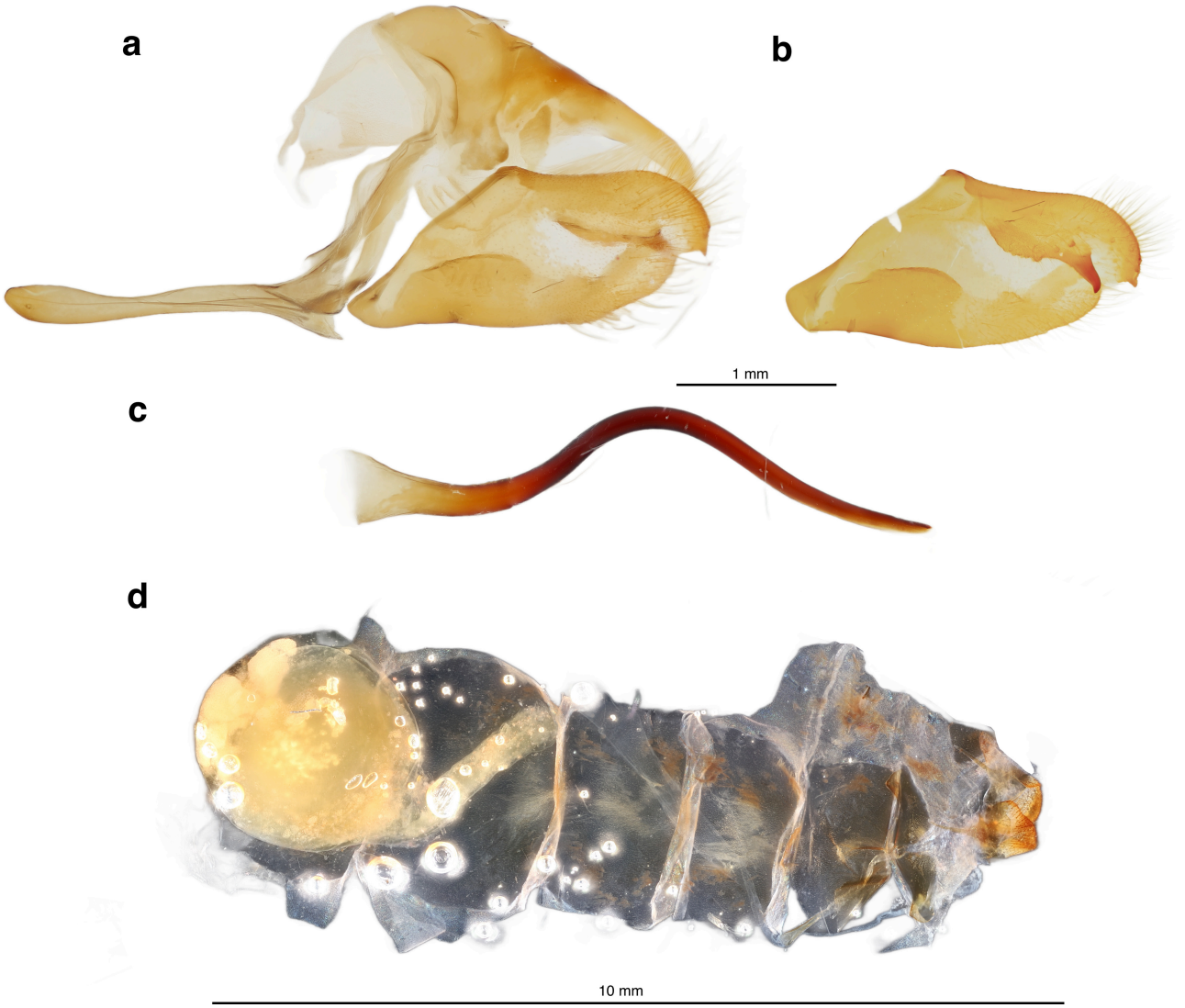

FIGURE 7. Male and female genitalia of *Colobura cryptica* **sp. nov.** a. lateral view of male genitalia with aedeagus removed, b. inner lateral view of valva, c. lateral view of aedeagus, d. lateral view of female genitalia with abdominal segments (reference scale: 1 mm for male genitalia, 10 mm for female genitalia).

Results

Explanation of the phylogenetic trees

The phylogenetic trees constructed using the autosomes from the nuclear genome (Fig. 8), from genes predicted to be in the Z chromosome (Fig. 9), and from the mitochondrial genome (Fig. 10), reveal four clusters corresponding to those initially present in COI barcode data in BOLDSystems (2025) (Fig. 3). All phylogenetic trees, including the COI barcode phylogenetic tree (see Supplements 2 and 3), reveal two primary clusters for *C. dirce* populations, separated by the Andes mountain range. The western clade comprises populations from Central America, the Caribbean, and west of the Andes, while the eastern clade includes populations from southern Ecuador, Colombia, Venezuela, and areas southward (Figs. 3, 8–10). Here we revise the distribution of the *C. dirce dirce* and *C. dirce wolcotti*, with *C. dirce dirce* comprising the eastern clade and *C. dirce wolcotti* comprising the western clade. Specimens of *C. dirce wolcotti* and *C. dirce dirce* showed patterns of UV reflectance in agreement with our initial expectations (strongly expressed in Caribbean populations, highly variable from Mexico to Panama and in coastal Ecuador/northern Colombia west of the Andes and markedly reduced or absent in populations east of the Andes).

FIGURE 8. Phylogenetic tree constructed from protein-coding regions of nuclear genome of genus *Colobura*.

FIGURE 9. Phylogenetic tree constructed from protein-coding regions predicted to be located in the Z chromosome of genus *Colobura*.

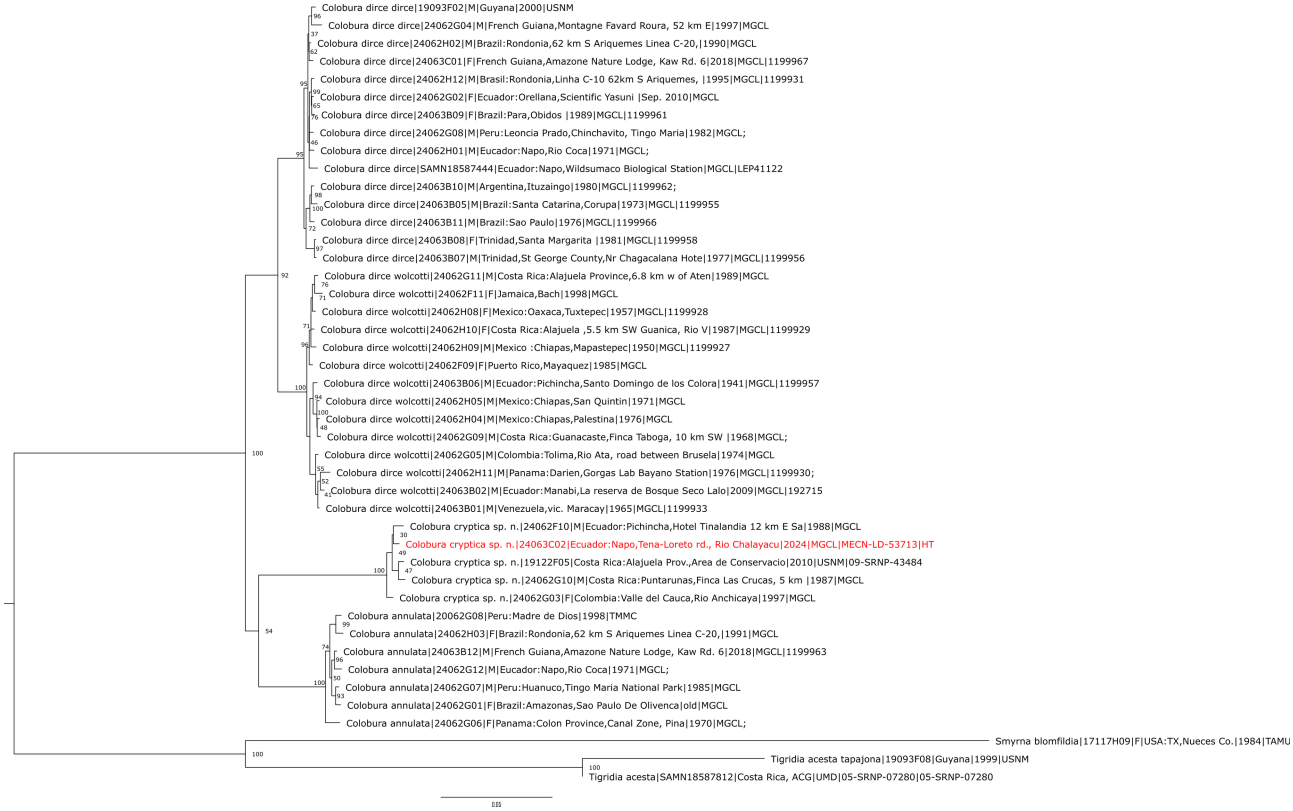

FIGURE 10. Phylogenetic tree constructed from protein-coding regions in mitochondrial genome of genus *Colobura*.

A third cluster contains specimens with typical *C. annulata* morphology, where the third submarginal line from the distal margin in the ventral forewing crosses vein M_3 and touches the transverse yellow band (Fig. 2b), matching the holotype of *C. annulata*. The fourth cluster also has typical *C. annulata* morphology except that the third submarginal line on the ventral forewing does not cross vein M_3, or if it crosses it, it appears faded (Fig. 2c). Larval rearing confirmed that caterpillars lacking both yellow lateral spots and yellow rings developed into adults with wing patterns matching those of sequenced specimens in the fourth clade. This cluster is described here as *Colobura cryptica* sp. nov.

Colobura cryptica sp. nov. Sapkota, Orellana & Willmott

Holotype: UF / FLMNH / MGCL 1218008 [green printed label] // ECUADOR: Napo / Tena-Loreto rd., Río Chalayacu / 1000 m, 0°43'3"S, 77°40'56"W / 5.xi.2024, Hall, J.P.W., Willmott, K.R. / MECN-LD# 53713 [white printed label] // DNA sample ID: / NVG-24063C02 / c/o Nick V. Grishin [white printed label] // DNA voucher / LEP-98811 [white printed label] // HOLOTYPE *Colobura cryptica* Sapkota, Orellana & Willmott, 2026 [red printed label] (1♂) (to be deposited in INABIO).

Eleven Paratypes: **ECUADOR**: Esmeraldas. Lita-San Lorenzo Road, NE San Francisco, ridge N La Ceiba, ii/2017, R. Aldaz, FLMNH 288578, DNA Voucher LEP-57412, MGCL (1.1325°N, 78.658889°W, 250m) (1♀); Pichincha. Hotel Tinalandia 12 km E Santo Domingo de los Colorados, v/9/1988, G. & A. Austin, NVG-24062F10, MGCL (failed) (2460 to 2800 ft) (1♂); Manabí. Pedernales-Jáma rd., Reserva Lalo Loor, M. F. Checa, 4329M, QCAZ (0.0913888°S, 80.14888°W). **COLOMBIA**: Valle del Cauca. Río Anchicayá, i/15/1997, S. & L. Steinhauser, NVG-24062G03, MGCL (3770 ft) (1♀); **COSTA RICA**. Alajuela. Área de Conservación Arenal, San Ramón, Villa Blanca 5, xii/1/2008, R. González Tenorio, ASARD4868-12, INBio (10.202°N, -84.485°W, 1050m); vii/1/2009, R. Rojas Valverde, ASARD4865-12, INBio (10.203°N, -84.483°W, 1050m) (1♀); Cartago. Área de Conservación La Amistad Pacífico, Paraíso, Sendero Pava Catarata 2, vii/1/2008, R. González Tenorio, ASARD4866-12+I97BA97: N99, INBio (9.736°N, -83.782°W, 1350) (1♂); Sendero Pava Catarata 1, viii/8/2008, R. González Tenorio,

ASARD4864-12, INBio (9.736°N, -83.783°W, 1350m) (1♀); Puntarenas. Finca Las Cruces, 5 km S San Vito de Java, ix/10/1987, G. & A. Austin, KW-24-68, NVG-24062G10, MGCL (1♂) (dissected); **VENEZUELA**. Táchira. San Cristóbal, Parque Nacional Natural Paramillo, iii/26/2023, A. Orellana, FUNEA (7.7931°N, -72.1949°W, 1100 m) (1♂); (1♀).

Description. Adult male. *Head*. Head length (from occiput to clypeus) 2.6 mm (n=3) and greatest head width (across eyes) 4.3 mm (n=3); frons creamy with a median transverse black stripe on each side; vertex blackish brown; antennal length (from base of scape to apex of club) 22–24 mm long (n=3); shaft brown; club black with pale dorsal apex; eyes brown, without setae; palpi outer side creamy, inner and dorsal sides dark brown; palpi obtusely angulate forward; proboscis dark brown.

Thorax. Thorax 10–11 mm long and c. 4–6 mm wide (n=3), dark brown with long dark brown hair-like scales dorsally; ventrally cream-colored with four lateral stripes which are extensions of wing stripes; legs dorsally dark brown, ventrally cream-colored.

Legs. Tarsal formula male, 2-5-5; female, 4-5-5. **Forelegs** relatively reduced, shortest: femur, tibia, and tarsi smooth in male; tarsi with sparse inner spines in female, two elongate tarsal spines extended as claws along with elongate hair-like setae. **Midlegs** slightly shorter than hindlegs: femur longer than tibia, smooth; tibia with sparse inner spines; tarsi subequal to tibia, with dense rows of inner spines; two arcuate claws; elongate hair-like setae present between and around claws; pulvillus circular pad-like medially, biforked at margins as partially sclerotized claw-like structures. **Hindlegs** slightly longer than midlegs: femur smooth; tibia longer than femur, with sparse inner spines; tarsi subequal to tibia, heavily spined as in midlegs; claws and pulvilli as in midlegs.

Wings. Forewing length (center of mesothorax to wing apex) 36–40 mm (n=3). Male (average forewing length 38 mm, n=2) forewing triangular with straight distal margin; hindwing triangular with produced tornal lobe. **Dorsal surface**. Forewing ground color dark blackish brown; cream-colored postdiscal band extending from costa to near tornus, almost to vein 1A+2A, with relatively smooth edges; basal area dark brown, apical area blackish brown; Hindwing ground color dark brown, becoming blackish brown in marginal area; cream-colored costal band extending from wing base to apex. **Ventral Surface**. Forewing ground color cream, except for cell 1A + 2A which has gray ground color and CuA_2 where cream color only enters anterior portion, about 1/3rd of cell; discal cell with dark spot at base, followed by four dark brown transverse lines, distal 3rd and 4th are joined at costa; base of cell CuA_2-CuA_1 has a blackish brown spot, followed distally by a dark brown transverse line; slightly pale cream-colored postdiscal band as on dorsal surface; postdiscal band bordered distally from vein M_2 to costa by dark brown line; distal of this line two dark brown postdiscal lines, parallel to each other, extending respectively from costa to R_5 and costa to vein M_1; four dark brown transverse submarginal lines, almost parallel to each other and margin, basal-most even in width, extending from vein R_3 straight to M_2, then curving facing margin to terminate in mid M_3-CuA_1, third from margin even in width, extending from costa to vein M_3, faded at distal end, second from margin straight, extending and broadening very slightly but continuously ending at mid M_3-CuA_1, and that closest to margin extending from costa to cell CuA_2-M_3, broadening slightly between veins M_3 to CuA_1 where it ends; thin dark brown marginal border, narrowing gradually from apex to tornus. Hindwing ground color cream; dark brown line bordering costa; dark brown spot at base of humeral vein; seven dark brown transverse lines in cell Rs-Sc+R_1, first starting slightly above vein Sc+R_1 and ending slightly above vein Rs, second starting above vein Sc+R_1, ending at Rs, third starting from costa and ending before Rs, fourth and fifth and sixth and seventh joining at costal margin and ending midway cell Sc+R_1-Rs; dark brown line at base of discal cell extending to anal margin; 10 longitudinal dark brown lines extending into wings from anal margin, first two entering and crossing discal cell, third reaching base of vein CuA_1 and bending sharply towards tornus to meet eighth line from anal margin, fourth line extending to CuA_2 and then bending sharply basally to run parallel to vein CuA_2 to meet seventh line from anal margin, 5th extending to vein 1A+2A then bending sharply basally and again making a U-turn to run parallel to vein 1A+2A and end just before 4th horizontal line, 6th extending to vein 1A+2A, 9th and 10th extending across posterior half of cell CuA_2, discal and post discal area with total of seven transverse brown lines, first proximal, dark brown, extending midway of posterior vein M_1–M_2 to CuA_2, second dark brown line arising midway from cell Rs and ending midway cell CuA_1–CuA_2, remaining 5 brown lines all arising from Rs, tapering and converging in cell M_3-CuA_1 and vanishing, 4th and 5th from distal end, joining at Rs vein, 5th has a blue pupil; black submarginal line starting at posterior end of cell Rs-M_1 and ending at vein CuA_2; thin marginal line dark brown starting midway Rs-M1 ending at tornus; two diffuse orange elongated patches, on either side of distal vein CuA_2, above having dark brown spot at base, lower one reaching tornal spots; two partly fused black tornal spots in cell 1A+2A-Cu_2 with blue pupil in one nearest to CuA2; no hair

pencils or scent gland. Adult female. Externally similar to male except slightly broader wings (forewing length=39 mm, n=1)

Abdomen. Both sexes. Abdomen 13 mm long (n=3), dorsal and lateral sides dark brown; ventral side cream-colored with black longitudinal stripes on each side.

Genitalia. Adult male. Uncus slender, curved inward apically; costal margin of valva slightly depressed at midpoint, terminating posteriorly in a small ventrally directed 'beak'; clasper, arising from inner flap of costal valva, sclerotized, ventrally directed, hooked; aedeagus heavily sclerotized, strongly curved at mid-point. Adult female. Papillae anales sclerotized, with outward projected hairs, each semicircular, join to form narrow opening, apophyses posteriores shorter than papillae anales; ductus bursae as long as abdomen, filamentous, corpus bursae broadly oval, membranous, no signum, ductus seminalis arising from anterior region of ductus bursae, lamella post vaginalis formed of two roughly triangular lateral plates fused around ostium bursae and with dorso-anterior corners extending as rounded lobes inside posterior edge of seventh sternite.

Diagnosis. (Figs. 2 a–c). Ventral forewing with third dark brown submarginal line from distal margin of even thickness throughout (unlike in *C. dirce* which is swollen posteriorly) and ending at vein M_3, or if it crosses vein M_3, it is faded and ends at middle of cell M_3-CuA_1 (unlike *C. annulata* where the line reaches to the transverse band). Ventral forewing with dark brown spot in cell M_1-R_5 small, of equal width to spot adjacent at costa in cell R_4-R_3 (as in *C. annulata*, whereas in *C. dirce* the distal spot is broader); dorsal forewing with distal edge relatively smooth (as in *C. annulata*, whereas in *C. dirce* distal edge of cream band often "kinked" at vein M_3); dorsal forewing with pale band of even width throughout (as in *C. annulata*, whereas in *C. dirce* the band often narrows at the costa). Specimens with the shorter third dark brown submarginal line on the ventral forewing, typical of *C. cryptica,* are known from Costa Rica, Colombia (from Valle de Cauca), Venezuela (from Táchira), and eastern Ecuador (and potentially other areas in the lowland Amazon); however, a single barcoded individual from eastern Ecuador (from Yasuní Scientific Station) proved to be a form of *C. annulata*. Additional barcoding is needed to better determine the range of variation in wing pattern within *C. annulata*, but, minimally, the diagnostic characters identified above seem to be valid within the distribution of barcoded specimens of *C. cryptica*.

Etymology. Although *Colobura* are among the most common Neotropical butterflies, realizing the true species diversity within this genus has proven challenging owing to cryptic morphological characters. The new species *C. cryptica* **sp. nov.** is very similar to its congeners *C. dirce* and *C. annulata* in larval and particularly in adult morphology, except for several subtle characters. The specific epithet is a feminine Latin adjective meaning hidden or concealed, given in allusion to the cryptic identification features of this species.

Biology. *Colobura cryptica* occurs from sea level up to elevations of at least 1,350 m and perhaps as high as 1,800 m. In Venezuela, larvae are gregarious, typically found in clusters of around 30 individuals on the undersides of leaves. AO observed one such batch on a *Cecropia* tree less than 4 m tall, growing in secondary growth within mature humid premontane forest. The caterpillars exhibited highly synchronous development, molting and pupating at the same time. Adult eclosion occurred within approximately 15 days of pupation. The pupae measured up to 40 mm in length (n=1) and resembled dried tree bark. They are cylindrical, tapering gradually from the head to the cremaster, with the widest point (6.5 mm) at the thorax. The surface is pale brown, marked with irregular projections and dark warts that enhance the bark-like appearance. Early instar larvae fed collectively and chewed through the primary veins of the leaves, causing the blades to fold in a "closed umbrella" fashion. This behavior likely reduces sap flow and may facilitate feeding or help circumvent plant defenses or provide the larvae with protection from predation. Similar behavior has been observed in *C. dirce* (pers. obs.). In Venezuela, adults of *C. cryptica* are found throughout the year. The holotype male of *C. cryptica* was attracted to rotting fish liquid on the ground beside a wide, forested mountain river at 1:30 pm in Napo, Ecuador. Isidro Chacón (IC) used rotting fruit baits to attract and collect adults in the Caribbean side of Costa Rica.

Distribution. *Colobura cryptica* occurs from Chiapas in eastern Mexico to Panama in Central America, and in northwestern South America, west of the Andes in Colombia and Ecuador, and along the east Andean foothills from Venezuela to southern Ecuador. Specimens with ventral wing patterns similar to the holotype of *C. cryptica* have also been photographed at scattered localities in Amazonian Brazil and southern Peru (inaturalist.org), but to date no barcoded specimens are available to confirm this distribution (see Diagnosis above) (Fig. 14).

Key to species and subspecies identification in adults of *Colobura*

1. Ventral forewing with third dark brown submarginal line swollen in cells M_1-M_3; dark brown spot in cell M_1-R_5, oval shaped, broader than adjacent spot at costa in cell R_4-R_3; dorsal forewing with pale band often narrowing at costa 2

- Ventral forewing with third dark brown submarginal line not swollen in cells M_1-M_3; dark brown spot in cell M_1-R_5 small, of equal width to spot adjacent at costa in cell R_4-R_3; dorsal forewing with pale band of even width throughout 3

2. Ventral wings do not have distinctly visible violet to UV reflectance; continental South America east of Andes . . . . . *C. dirce dirce*

- Ventral wings have very distinct violet to UV reflectance; Caribbean and locations west of Andes . . . . . *C. dirce wolcotti*

3. Ventral forewing with third dark brown submarginal line reaching cream-yellow transverse band . . . . . *C. annulata*

- Ventral forewing with third dark brown submarginal line not reaching cream-yellow transverse band . . . . . *C. cryptica*

Key to species identification in larvae of *Colobura*

1. Body with cream-yellow rings at posterior edge of A_1 to A_7 segments . . . . . *C. annulata*
- Body without cream-yellow rings between each abdominal segment 2
2. Vertically elongate lateral cream-yellow spots at anterior edge of abdominal segments; head horns and thoracic scoli whitish gray, remaining scoli pale yellow . . . . . *C. dirce*
- Abdominal segments entirely black, lacking cream-yellow lateral spots; head horns and all scoli deep yellow . . . . . *C. cryptica*

Genitalic morphology

No consistent differences in the male and female genitalia among all four genetic clusters were found (Figs. 4–7).

Geographical distribution of congeners

Colobura dirce dirce. Distributed east of the Andes from Venezuela to Bolivia, Brazil, northeastern Argentina, Paraguay, the Guianas and Trinidad (Fig. 11).

Colobura dirce wolcotti. Distributed from central Mexico to southwestern Ecuador, west of the Andes in Colombia and Venezuela, and in the Greater Antilles (Fig. 12).

Colobura annulata. Distributed from Honduras to western Ecuador, Venezuela to Bolivia, Amazonian Brazil, the Guianas, and Trinidad (Fig. 13).

UV reflectance study

Specimens of *Colobura dirce dirce* (n=13) and *C. d. wolcotti* (n=12) differed in mean peak reflectance. *C. d. dirce* showed a peak at 362.2 nm (±7.88 SD), whereas *C. d. wolcotti* peaked at 390.6 nm (±12.38 SD) (Fig. 15a–b). The latter also exhibited slightly higher UV reflectance intensity at its mean peak wavelength (30%) compared to *C. d. dirce* (27%). The more pronounced violet shimmer in *C. d. wolcotti* visible to humans is a result of the peak wavelength being closer to the violet edge of human vision (around 400 nm). However, a Dunn post hoc test indicated no significant difference in peak wavelength between these two taxa ($p=0.6901 > 0.01$).

For *C. annulata* (n=7), the reflectance peak was 369.7 nm (±6.3 SD) with around 27% reflectance, while *C. cryptica* (n=4) peaked at 343.8 nm (±4.8 SD) with around 18% reflectance (Fig. 15c–d). Across all species, reflectance spectra displayed considerable intraspecific variation. Although most pairwise comparisons were not significant, the Dunn post hoc test revealed a significant difference in mean peak wavelength between *C. d. dirce* and *C. cryptica* (p-value=0.00627 <0.01, difference=18.4 nm).

FIGURE 11. Distribution map of *Colobura dirce dirce,* stars represent the localities from where specimens were collected for molecular analysis.

FIGURE 12. Distribution map of *Colobura dirce wolcotti,* stars represent the localities from where specimens were collected for molecular analysis.

To further assess sympatric populations, we compared specimens from Napo, Ecuador, where *C. cryptica* (n=1), *C. d. dirce* (n=1), and *C. annulata* (n=1) occur together. The spectra (Fig. 16) show clear separation in both peak wavelength and percent reflectance: *C. cryptica* ~330 nm, *C. annulata* ~356 nm, and *C. d. dirce* ~359 nm, consistent with broader patterns observed above.

FIGURE 13. Distribution map of *Colobura annulata,* stars represent the localities from where specimens were collected for molecular analysis.

FIGURE 14. Distribution map of *Colobura cryptica* **sp. nov.,** stars represent the localities from where specimens were collected for molecular analysis and blue star represent the holotype locality and question marks represent the possible distribution.

Discussion

Based on type localities, the western populations of *Colobura dirce* correspond to *Colobura dirce wolcotti* (type locality: Puerto Rico) and the eastern populations to *C. d. dirce* (type locality: French Guiana). The absence of sympatry among haplotypes within each cluster, their relatively low genetic divergence compared to that observed among sympatric *Colobura* species, and the lack of consistent morphological differences, all support treating these lineages as subspecies rather than distinct species. *Colobura cryptica* shows substantial genetic divergence and

consistently forms a distinct clade in all phylogenetic analyses. Morphological traits further support its distinctiveness, and its sympatry with *C. annulata* confirms that it should be recognized as a valid species.

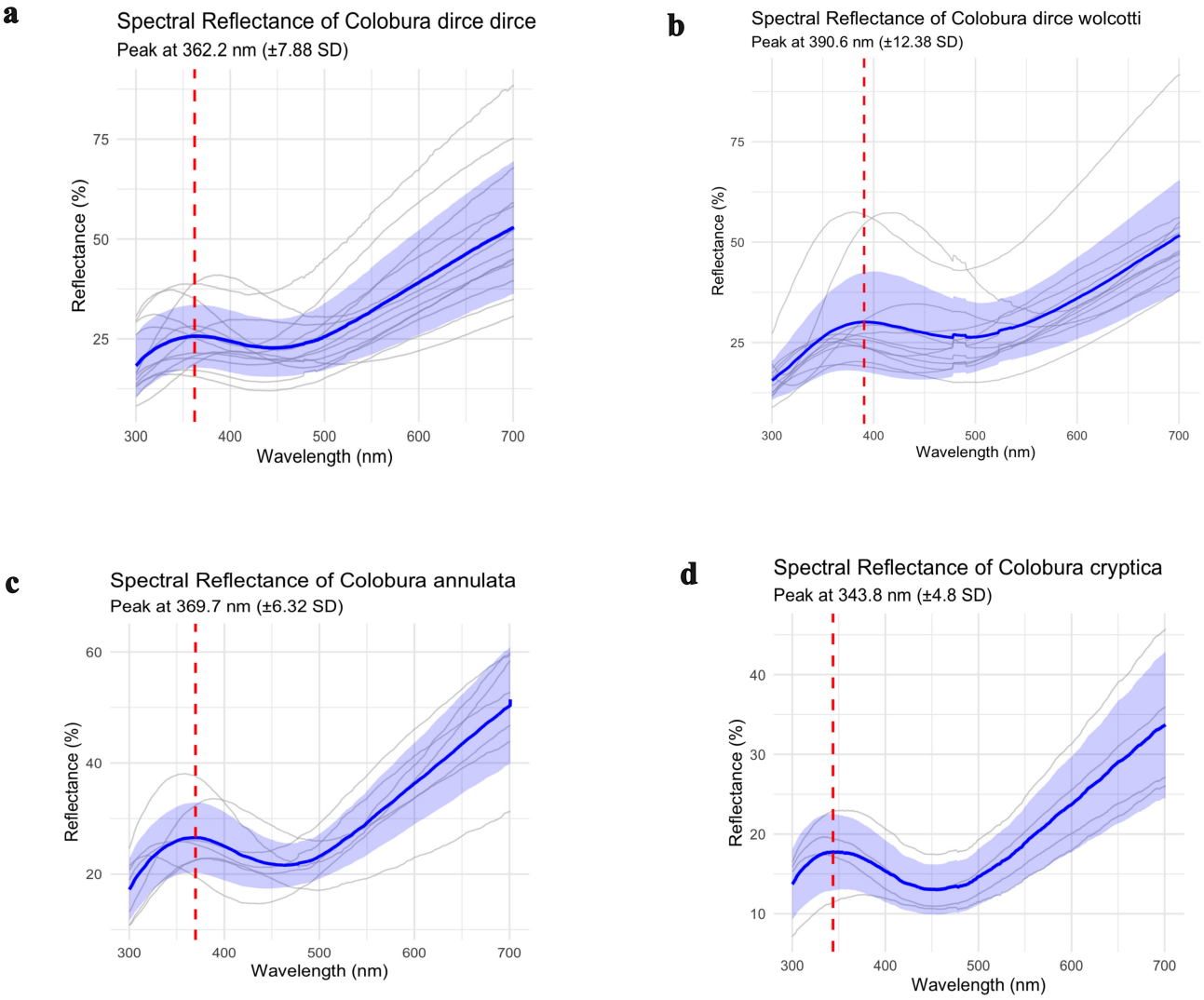

FIGURE 15. Reflectance spectra of *Colobura* species, showing percent reflectance (y-axis) across wavelengths (x-axis, 300 to 700nm). The blue curve shows the mean reflectance for each species; the shaded ribbons indicate the standard deviation. Dashed red vertical lines show the wavelength (between 300 to 400) at which the species exhibits maximum mean reflectance. a. *Colobura dirce dirce* b. *Colobura dirce wolcotti* c. *Colobura annulata* and d. *Colobura cryptica*.

We did not detect any significant differences in genitalia morphology in either males or females, despite these traits being the primary characters traditionally used to infer reproductive isolation in cryptic species (Tuxen, 1970; Hosken & Stockley, 2004; Song & Bucheli, 2010; Masly, 2012). Moreover, none of the taxa possess hair pencils or known androconial glands, suggesting that pheromonal cues are unlikely to play a major role in mate recognition in *Colobura*. Instead, our UV reflectance analyses suggest a plausible alternative prezygotic isolation mechanism (cf. Meyer-Rochow, 1991; Lukhtanov *et al*. 2005; Imafuku, 2008 in lycaenids; Silberglied & Taylor, 1973; Allyn & Downey, 1977 in pierids; Finkbeiner *et al*. 2017; Dell'Aglio *et al*. 2018 in *Heliconius*).

The spectral properties of *Colobura* fall within the range of known butterfly visual sensitivity in UV region: males of *Heliconius erato* (Linnaeus, 1758) (λmax=360 nm; McCulloch *et al*. 2016), *Vanessa cardui* (Linnaeus, 1758) (λmax=360 nm; Chen, 1987), *Polygonia c-album* (Linnaeus, 1758) (λmax=350 nm; Vanhoutte & Stavenga, 2005), and *Danaus plexippus* (Linnaeus, 1758) (λmax=340 nm; Stalleicken *et al*. 2006) (reviewed in Van der Kooi *et al*. 2021). These λmax values are likely sufficient to serve as reliable cues for species recognition and mate choice. The three species of *Colobura* exhibit distinct peak UV wavelengths. A statistically significant difference of λmax=18 nm was detected between *C. d. dirce* and *C. cryptica*, despite the wide geographic range of specimens

examined (Mexico to Brazil and Argentina), the inclusion of both sexes, and variation in specimen age. Effects of age and environment on UV reflectance have been reported in other butterflies: Kemp (2006) in *Colias eurytheme* Boisduval, 1852, Kemp and Macedonia (2006) in *Hypolimnas bolina* (Linnaeus, 1758), and Stella *et al*. (2018) in *Pieris napi* (Linnaeus, 1758), and may have influenced our other comparisons among *Colobura* species. We also found preliminary evidence for differences in UV reflectance among single specimens of *C. d. dirce*, *C. annulata* and *C. cryptica* from eastern Ecuador, consistent with a possible role for this trait in maintaining reproductive isolation. Whether these spectral traits remain stable across additional specimens, geography and seasons, or instead vary locally, will require further sampling. Similar spectral differences have been observed in other butterflies; for example, Piszter *et al*. (2021) demonstrated concordance between spectral properties and population genetic structure in *Polyommatus icarus* (von Rottemburg, 1775), where eastern and western European populations differed by λmax=20 nm. In our sympatric population from Napo, Ecuador, the divergence between *C. cryptica* (n=1) and *C. annulata* (n=1) was even greater, with λmax differing by 25 nm.

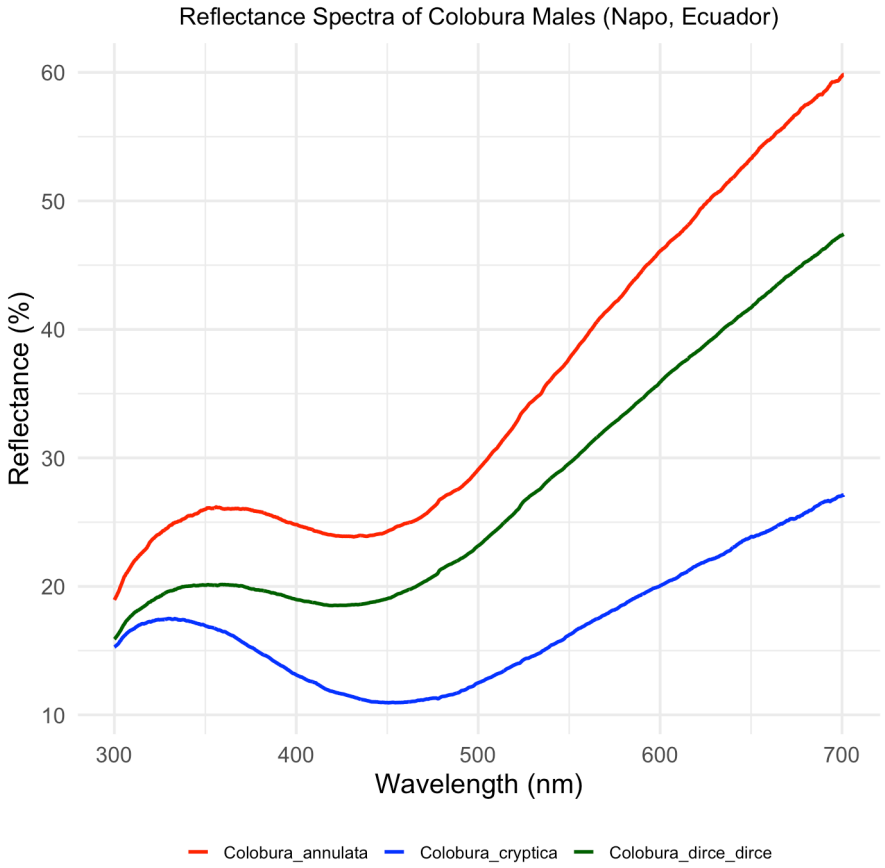

FIGURE 16. Reflectance spectra of male *Colobura* species, showing percent reflectance (y-axis) across wavelengths (x-axis, 300 to 700nm) for species found in Napo, Ecuador. Red line shows reflectance spectra of *Colobura annulata*, green shows that of *Colobura dirce dirce* and blue shows that of *Colobura cryptica*.

Data from bait-trapping experiments conducted by DeVries *et al*. (1999) and later reexamined by Willmott *et al*. (2001) revealed significant differences in vertical stratification between *Colobura dirce* and *C. annulata* in lowland primary forests of eastern Ecuador near Añangu. Specifically, *C. d. dirce* tended to occupy the shaded understory, whereas *C. annulata* was more frequently associated with the sunlit canopy. In contrast, Mena *et al*. (2020) found no significant differences in vertical stratification between the two species in the Ecuadorian Chocó rainforest in northern Ecuador. These conflicting results may reflect differences in methodological approaches, and the absence of comparable data for *C. cryptica* further complicates interpretation. Nonetheless, the occurrence of taxa with distinct spectral properties in habitats differing in light environment may facilitate species recognition and mate selection. Although ecological data and behavioral experiments are needed to directly test this hypothesis, the combined ecological, morphological, and optical evidence suggests that further investigation of the role of UV reflectance in promoting reproductive isolation among sympatric *Colobura* species could be worthwhile.

Conclusion

Our integrative analyses reveal that *Colobura* comprises four distinct lineages, including *C. cryptica* sp. nov., which is genetically and morphologically distinct from its sympatric sister species *C. annulata*. A biogeographical split in *C. dirce* populations across the Andes was documented, and the ranges of *C. dirce wolcotti* and *C. dirce dirce* were redefined. Genome sequencing showed that the name *C. d. wolcotti*, previously applied to individuals from the Caribbean Islands, should be expanded to also include populations from Central America and coastal Ecuador/northern Colombia west of the Andes, whereas *C. d. dirce* occurs only east of the Andes. The eastern and western populations of *C. dirce* are interpreted as subspecies, reflecting low genetic divergence and minor morphological differences. UV reflectance patterns were found to differ among species and are likely to serve as visual cues for species recognition and mate selection, potentially contributing to reproductive isolation. Combined with observed ecological segregation, particularly vertical stratification in forest habitats, these findings highlight the role of subtle morphological, spectral, and ecological traits in maintaining species boundaries and underscore the value of integrative approaches in uncovering cryptic biodiversity in Neotropical butterflies.

Acknowledgments

We are grateful to the McGuire Center for Lepidoptera and Biodiversity (MGCL), Gainesville, Florida, for access to specimens and research facilities, and to Andrew Neild for providing photographs of the neotype and holotype of *Colobura dirce* and *C. annulata*. We thank Jonathan Bremer at the Florida State Collection of Arthropods (FSCA), Gainesville, Florida, for access to genitalia imaging equipment. We acknowledge the Texas Advanced Computing Center (TACC) at the University of Texas at Austin for providing high-performance computing resources, and Jinhui Shen, Jing Zhang, and Qian Cong at the University of Texas Southwestern Medical Center, Dallas, Texas, for their assistance with DNA extraction and computational analyses. The genomics computation was supported in part by Howard Hughes Medical Institute Investigator funds to N.V. Grishin and by grants from the National Institutes of Health (GM127390) and the Welch Foundation (I-1505) to N.V. Grishin. Collections by D.H. Janzen and W. Hallwachs were made possible through awards from Canada's New Frontiers in Research Fund (NFRFT-2020-00073) and the Canada Foundation for Innovation's Major Science Infrastructure program (MSI 42450). These programs sustained the analytical capacity and informatics platforms at the Centre for Biodiversity Genomics, University of Guelph, Canada, which support the BIOSCAN research program and its key initiatives, including BioAlfa and BOLD. We extend special thanks to the Walder Foundation (Chicago, USA) and the Government of Costa Rica for their contributions to these efforts. All yy-SRNP-nnnnn and DHJPAR-nnnnn vouchered specimens were collected, exported, and DNA-barcoded under Costa Rican government permits issued to BioAlfa (Janzen and Hallwachs, 2019): R-054-2022-OT-CONAGEBIO; R-019-2019-CONAGEBIO; National Published Decree #41767; JICASAPI #0328497 (2014); and D.H. Janzen and W. Hallwachs (ACGPI-036-2013; R-SINAC-ACG-PI-061-2021; Resolución Nº001-2004 SINAC; PI-028-2021). Fieldwork and immature studies by A.O. were supported by Project UNET 04-002-2022. We thank Sofía Nogales, Ana García, Diego J. Inclán, the Instituto Nacional de Biodiversidad (INABIO), and the Ecuadorian Ministerio del Ambiente, Agua y Transición Ecológica for arranging the necessary permits for research in Ecuador, most recently under the project "Study of the Genetic Diversity and Evolution of the Lepidoptera of Ecuador" (permit number MAATE-DBI-CM-2023-0298). We also thank parataxonomists from the Área de Conservación Guanacaste, as well as Raúl Aldaz, Jason Hall, and Fernanda Checa, for assistance in collecting and providing information on *Colobura* specimens. We are additionally grateful to Alexis López Hernández, Olivier Claessens, and Javier Villamil for granting permission to use their *Colobura* photographs from iNaturalist. A.S. and S.K.C. are especially thankful to their advisor, Vaughn M. Shirey, for providing access to UV equipment used in this study, and A.S. further thanks Juliette Rubin for training in spectrophotometer measurement techniques. Finally, the authors thank the McGuire Student Publication Fund for financial support toward the publication of this work.

References

Allyn, A.C. & Downey, J.C. (1977) *Observations on male UV reflectance and scale ultrastructure in Phoebis (Pieridae)*. The Allyn Museum of Entomology, Sarasota, Florida, 20 pp.

BOLDSystems. (2025) Barcode of Life Data System. Version 4. Available from: https://www.boldsystems.org (accessed 3 November 2025)
Briscoe, A.D., Bybee, S.M., Bernard, G.D., Yuan, F., Sison-Mangus, M.P., Reed, R.D., Warren, A.D., Llorente-Bousquets, J. & Chiao, C. (2010) Positive selection of a duplicated UV-sensitive visual pigment coincides with wing pigment evolution in *Heliconius* butterflies. *Proceedings of the National Academy of Sciences of the United States of America*, 107 (8), 3628–3633.
https://doi.org/10.1073/pnas.0910085107
Chazot, N., Wahlberg, N., Freitas, A.V.L., Mitter, C., Labandeira, C., Sohn, J.C., Sahoo, R.K., Seraphim, N., de Jong, R. & Heikkilä, M. (2019) Priors and Posteriors in Bayesian Timing of Divergence Analyses: The Age of Butterflies Revisited. *Systematic biology*, 68 (5), 797–813.
https://doi.org/10.1093/sysbio/syz002
Chen, D.M. (1987) Ultraviolet sensitivity in compound eye of the butterfly *Vanessa cardui*. *Acta Entomologica Sinica*, 30 (4), 353–358.
Cong, Q., Zhang, J. & Grishin, N.V. (2019) Genomic determinants of speciation. *bioRxiv*.
https://doi.org/10.1101/837666
Cong, Q., Shen, J., Zhang, J., Li, W., Kinch, L.N., Calhoun, J.V., Warren, A.D. & Grishin, N.V. (2021) Genomics reveals the origins of historical specimens. *Molecular Biology and Evolution*, 38 (5), 2166–2176.
https://doi.org/10.1093/molbev/msab013
Dayrat, B. (2005) Towards integrative taxonomy. *Biological journal of the Linnean society*, 85 (3), 407–417.
https://doi.org/10.1111/j.1095-8312.2005.00503.x
Davey, J.W., Chouteau, M., Barker, S.L., Maroja, L., Baxter, S.W., Simpson, F., Merrill, R.M., Joron, M., Mallet, J., Dasmahapatra, K.K. & Jiggins, C.D. (2016) Major improvements to the *Heliconius melpomene* genome assembly used to confirm 10 chromosome fusion events in 6 million years of butterfly evolution. *G3: Genes, Genomes, Genetics*, 6 (3), 695–708.
https://doi.org/10.1534/g3.115.023655
Dell'Aglio, D.D., Troscianko, J., McMillan, W.O., Stevens, M. & Jiggins, C.D. (2018) The appearance of mimetic *Heliconius* butterflies to predators and conspecifics. *Evolution; international journal of organic evolution*, 72 (10), 2156–2166.
https://doi.org/10.1111/evo.13583
DeVries, P.J., Walla, T.R. & Greene, H.F. (1999) Species diversity in spatial and temporal dimensions of fruit-feeding butterflies from two Ecuadorian rainforests. *Biological Journal of the Linnean Society*, 68 (3), 333–353.
https://doi.org/10.1111/j.1095-8312.1999.tb01175.x
Fenner, J., Rodriguez-Caro, L. & Counterman, B. (2019) Plasticity and divergence in ultraviolet reflecting structures on Dogface butterfly wings. *Arthropod Structure & Development*, 51, 14–22.
https://doi.org/10.1016/j.asd.2019.06.001
Finkbeiner, S.D., Fishman, D.A., Osorio, D. & Briscoe, A.D. (2017) Ultraviolet and yellow reflectance but not fluorescence is important for visual discrimination of conspecifics by *Heliconius erato*. *Journal of Experimental Biology*, 220 (7), 1267–1276.
https://doi.org/10.1242/jeb.153593
Hosken, D.J. & Stockley, P. (2004) Sexual selection and genital evolution. *Trends in ecology & evolution*, 19 (2), 87–93.
https://doi.org/10.1016/j.tree.2003.11.012
Imafuku, M. (2008) Variation in UV light reflected from the wings of *Favonius* and *Quercusia* butterflies. *Entomological Science*, 11 (1), 75–80.
https://doi.org/10.1111/j.1479-8298.2007.00247.x
iNaturalist. (2025) Observations of *Colobura* from the Americas. Available from: https://www.inaturalist.org (accessed 3 November 2025)
Kemp, D.J. (2006) Heightened phenotypic variation and age-based fading of ultraviolet butterfly wing coloration. *Evolutionary Ecology Research*, 8 (3), 515–527.
Lukhtanov, V.A., Kandul, N.P., Plotkin, J.B., Dantchenko, A.V., Haig, D. & Pierce, N.E. (2005) Reinforcement of pre-zygotic isolation and karyotype evolution in *Agrodiaetus* butterflies. *Nature*, 436 (7049), 385–389.
https://doi.org/10.1038/nature03704
Masly, J.P. (2012) 170 years of "lock-and-key": Genital morphology and reproductive isolation. *International Journal of Evolutionary Biology*, 2012, 247352.
https://doi.org/10.1155/2012/247352
McCulloch, K.J., Osorio, D. & Briscoe, A.D. (2016) Sexual dimorphism in the compound eye of *Heliconius erato*: A nymphalid butterfly with at least five spectral classes of photoreceptor. *Journal of Experimental Biology*, 219 (15), 2377–2387.
https://doi.org/10.1242/jeb.136523
Mena, S., Kozak, K.M., Cárdenas, R.E. & Checa, M.F. (2020) Forest stratification shapes allometry and flight morphology of tropical butterflies. *Proceedings of the Royal Society B*, 287 (1937), 20201071.
https://doi.org/10.1098/rspb.2020.1071
Meyer-Rochow, V.B. (1991) Differences in ultraviolet wing patterns in the New Zealand lycaenid butterflies *Lycaena salustius*, *L. rauparaha* and *L. feredayi* as a likely isolating mechanism. *Journal of the Royal Society of New Zealand*, 21 (2), 169–177.
https://doi.org/10.1080/03036758.1991.10431405

Nguyen, L.T., Schmidt, H.A., Von Haeseler, A. & Minh, B.Q. (2015) IQ-TREE: a fast and effective stochastic algorithm for estimating maximum-likelihood phylogenies. *Molecular biology and evolution*, 32 (1), 268–274. https://doi.org/10.1093/molbev/msu300

Obara, Y., Ozawa, G., Fukano, Y., Watanabe, K. & Satoh, T. (2008) Mate preference in males of the cabbage butterfly, *Pieris rapae crucivora*, changes seasonally with the change in female UV color. *Zoological Science*, 25 (1), 1–5. https://doi.org/10.2108/zsj.25.1

Piszter, G., Kertész, K., Sramkó, G., Krízsik, V., Bálint, Z. & Biró, L.P. (2021) Concordance of the spectral properties of dorsal wing scales with the phylogeographic structure of European male *Polyommatus icarus* butterflies. *Scientific Reports*, 11 (1), 16498. https://doi.org/10.1038/s41598-021-95881-z

Ratnasingham, S. & Hebert, P.D.N. (2013) A DNA-based registry for all animal species: The Barcode Index Number (BIN) system. *PLoS ONE*, 8 (8), e66213. https://doi.org/10.1371/journal.pone.0066213

Schlick-Steiner, B.C., Steiner, F.M., Seifert, B., Stauffer, C., Christian, E. & Crozier, R.H. (2010) Integrative taxonomy: a multisource approach to exploring biodiversity. *Annual review of entomology*, 55 (1), 421–438. https://doi.org/10.1146/annurev-ento-112408-085432

Shorthouse, D.P. (2010) SimpleMappr, an online tool to produce publication-quality point maps. Available from: https://www.simplemappr.net (accessed 6 October 2025)

Silberglied, R.E. & Taylor, O.R. (1973) Ultraviolet differences between the sulphur butterflies, *Colias eurytheme* and *C. philodice*, and a possible isolating mechanism. *Nature*, 241 (5389), 406–408. https://doi.org/10.1038/241406a0

Silberglied, R.E. & Taylor, O.R. (1978) Ultraviolet reflection and its behavioral role in the courtship of the sulfur butterflies *Colias eurytheme* and *C. philodice* (Lepidoptera, Pieridae). *Behavioral Ecology and Sociobiology*, 3, 203–243. https://doi.org/10.1007/BF00296311

Song, H. & Bucheli, S.R. (2010) Comparison of phylogenetic signal between male genitalia and non-genital characters in insect systematics. *Cladistics*, 26 (1), 23–35. https://doi.org/10.1111/j.1096-0031.2009.00273.x

Stalleicken, J., Labhart, T. & Mouritsen, H. (2006) Physiological characterization of the compound eye in monarch butterflies with focus on the dorsal rim area. *Journal of Comparative Physiology A*, 192 (3), 321–331. https://doi.org/10.1007/s00359-005-0073-6

Stella, D., Pecháček, P., Meyer-Rochow, V.B. & Kleisner, K. (2018) UV reflectance is associated with environmental conditions in Palaearctic *Pieris napi* (Lepidoptera: Pieridae). *Insect Science*, 25 (3), 508–518. https://doi.org/10.1111/1744-7917.12429

Tuxen, S.L. (1970) *Taxonomist's glossary of genitalia in insects* (2nd ed.). Scandinavian University Press. https://doi.org/10.1163/9789004631663

Van Der Kooi, C.J., Stavenga, D.G., Arikawa, K., Belušič, G. & Kelber, A. (2021) Evolution of insect color vision: From spectral sensitivity to visual ecology. *Annual Review of Entomology*, 66 (1), 435–461. https://doi.org/10.1146/annurev-ento-061720-071644

Vanhoutte, K.J. & Stavenga, D.G. (2005) Visual pigment spectra of the comma butterfly, *Polygonia c-album*, derived from in vivo epi-illumination microspectrophotometry. *Journal of Comparative Physiology A*, 191 (5), 461–473. https://doi.org/10.1007/s00359-005-0608-x

Willmott, K.R., Simon, M., Ortiz-Acevedo, E. & Hall, J.P. (2017) First record of the enigmatic tribe Anaeomorphini (Lepidoptera, Nymphalidae, Charaxinae) outside of the Amazon basin: a new species of Anaeomorpha Rothschild, 1894, from the Chocó region of western Ecuador. *Insecta mundi*, 0548, 1–10.

Willmott, K.R., Constantino, L.M. & Hall, J.P.W. (2001) A review of Colobura (Lepidoptera: Nymphalidae) with comments on larval and adult ecology and description of a sibling species. *Annals of the Entomological Society of America*, 94 (2), 185–196. https://doi.org/10.1603/0013-8746(2001)094[0185:AROCLN]2.0.CO;2

Zhang, J., Cong, Q., Shen, J., Song, L. & Grishin, N.V. (2025) Advancing butterfly systematics through genomic analysis. The Taxonomic Report of the International Lepidoptera Survey, 12 (5), 1–201. https://doi.org/10.64338/im.1131.4aypc

Supplementary Materials. The following supporting information can be downloaded at the DOI landing page of this paper.

Supplement 1. List of voucher specimens with metadata used in molecular analyses, including locality and collection data, repository information, genitalia numbers, DNA sampling details, and GenBank accessions.

Supplement 2. COI barcode phylogeny of all the specimens that were used in this study.

Supplement 3. COI barcode sequence data of all the specimens that were used in this study.